PLOS PATHOGENS

RESEARCH ARTICLE

Protective efficacy of an attenuated *Mtb* ΔLprG vaccine in mice

Amanda J. Martinot[1,2], Eryn Blass[1☯], Jingyou Yu[1☯], Malika Aid[1], Shant H. Mahrokhian[1], Sara B. Cohen[3], Courtney R. Plumlee[3], Rafael A. Larocca[1], Noman Siddiqi[4], Shoko Wakabayashi[4], Michelle Gardner[4], Rebecca Audette[4], Anne Devorak[2], Kevin B. Urdahl[3,5], Eric J. Rubin[4], Dan H. Barouch[1,6]*

1 Center for Virology and Vaccine Research, Beth Israel Deaconess Medical Center, Harvard Medical School, Boston, Massachusetts, United States of America, **2** Department of Infectious Diseases and Global Health, Tufts University Cummings School of Veterinary Medicine, North Grafton, Massachusetts, United States of America, **3** Department of Immunology, Seattle Children's Research Institute, Seattle, Washington, United States of America, **4** Department of Immunology and Infectious Diseases, Harvard School of Public Health, Boston, Massachusetts, United States of America, **5** Departments of Pediatrics and Immunology, University of Washington, Seattle, Washington, United States of America, **6** Ragon Institute of MGH, MIT, and Harvard, Cambridge, Massachusetts, United States of America

☯ These authors contributed equally to this work.
* dbarouch@bidmc.harvard.edu

Citation: Martinot AJ, Blass E, Yu J, Aid M, Mahrokhian SH, Cohen SB, et al. (2020) Protective efficacy of an attenuated *Mtb* ΔLprG vaccine in mice. PLoS Pathog 16(12): e1009096. https://doi.org/10.1371/journal.ppat.1009096

Editor: Padmini Salgame, New Jersey Medical School, UNITED STATES

Received: June 7, 2020

Accepted: October 26, 2020

Published: December 14, 2020

Data Availability Statement: All relevant data are within the manuscript and its Supporting information files.

Funding: We acknowledge support from the National Institutes of Health (AI124377, AI126603, AI12875, BAA-NIAID-NIHAI201700104; D.H.B.), the National Institutes of Health (AI135098; A.J. M.), and the Ragon Institute of MGH, MIT, and Harvard (D.H.B.). The funders had no role in study design, data collection and analysis, decision to publish, or preparation of the manuscript. The authors declare no competing financial interests.

Abstract

Bacille Calmette-Guerin (BCG), an attenuated whole cell vaccine based on *Mycobacterium bovis*, is the only licensed vaccine against *Mycobacterium tuberculosis* (*Mtb*), but its efficacy is suboptimal and it fails to protect against pulmonary tuberculosis. We previously reported that *Mtb* lacking the virulence genes *lprG* and *rv1410c* (ΔLprG) was highly attenuated in immune deficient mice. In this study, we show that attenuated ΔLprG *Mtb* protects C57BL/6J, Balb/cJ, and C3HeB/FeJ mice against *Mtb* challenge and is as attenuated as BCG in SCID mice. In C3HeB/FeJ mice, ΔLprG vaccination resulted in innate peripheral cytokine production and induced high polyclonal PPD-specific cytokine-secreting $CD4^+$ T lymphocytes in peripheral blood. The ΔLprG vaccine afforded protective efficacy in the lungs of C3H/FeJ mice following both H37Rv and Erdman aerosolized *Mtb* challenges. Vaccine efficacy correlated with antigen-specific PD-1-negative $CD4^+$ T lymphocytes as well as with serum IL-17 levels after vaccination. We hypothesize that induction of Th17 cells in lung is critical for vaccine protection, and we show a serum cytokine biomarker for IL-17 shortly after vaccination may predict protective efficacy.

Author summary

Many successful vaccines are based on attenuated human pathogens. The only licensed tuberculosis vaccine, BCG, is based on an attenuated version of live whole cell *Mycobacterium bovis*, the causative agent of tuberculosis (TB) in cattle. Advantages to using attenuated pathogens as vaccines include a broad antigen composition including proteins, lipids, carbohydrates and other molecules that can induce durable immune responses

Competing interests: The authors have declared that no competing interests exist. A.J.M. and D.H. B. are co-inventors on a TB vaccine patent.

sometimes lasting decades. Here we test an attenuated *Mycobacterium tuberculosis (Mtb)*, the causative agent of human TB, that lacks a key virulence factor as an alternative whole cell vaccine in mice. Attenuated *Mtb* lacking a key virulence protein, LprG, is immunogenic and protects mice against *Mtb* challenge. The LprG whole cell vaccine is protective in mice that develop lung pathology more similar to what is described in human TB and the LprG vaccine induces a key cytokine, IL-17, thought to be important for vaccine protection, in the peripheral blood early after vaccination. Together these data support the continued development of attenuated TB as a potential vaccine candidate. Furthermore our data suggests that serum IL-17 should be explored as a potential biomarker for vaccine efficacy in preclinical animal models.

Introduction

BCG is currently the only approved TB vaccine for use in humans. While it protects against childhood TB meningitis, it provides only limited protection in adulthood [1]. Several BCG strains are available worldwide [2] and all are derived from attenuated strain *Mycobacterium bovis*, the mycobacterial agent of bovine tuberculosis. BCG attenuation is based on the loss of key virulence factors such as ESAT-6 and CFP-10 [3]. BCG vaccination is almost universal in high burden TB regions of the world. Therefore, any novel vaccination regimen should demonstrate, at a minimum, equivalent protective efficacy as BCG and ideally would surpass the protective benefit provided by BCG vaccination. Recent studies have suggested that boosting BCG with secondary doses of BCG or novel adjuvanted vaccines such as M72/AS01$_E$ may improve TB disease outcomes [4,5]. Data in non-human primates (NHP) showing the protective efficacy of prior *Mtb* infection on preventing subsequent acquisition of *Mtb* after re-exposure [6] coupled with recent clinical safety data on the use of attenuated whole cell *Mtb* vaccines suggest that the continued development of attenuated *Mtb* as TB vaccines is warranted [7].

Mycobacteria are characterized by a thick, lipid-rich cell wall composed of covalently bound peptidoglycan linked to arabinogalactan and mycolic acids [8,9]. Numerous non-covalently bound antigenic lipids are intercalated within the mycolic acid layer, many of which have been shown to play important roles in virulence and the host-pathogen interaction with *Mtb*. *Mtb* devotes a large portion of its genome to lipid synthesis and lipid export to maintain its elaborate cell wall structure. The genes *rv1411c-rv1410c*, encoding a lipoprotein (LprG) and transmembrane efflux pump (Rv1410), have been shown to be conditionally essential for *in vivo* survival in the murine model. Our previous work characterized this operon as a lipid transporter [10], disruption of which altered the lipid content of the *Mtb* cell wall and its metabolic state, leading to marked attenuation in both immunocompetent (C57BL/6J) and immunodeficient (*Rag* -/-, SCID, *phox* -/-, and *infr* -/-) mice [11].

The LprG lipoprotein is a potent TLR2 agonist [12] and has been hypothesized to play a role in host immune evasion by decreasing antigen presentation by macrophages *in vitro* [13]. LprG also binds immunomodulatory lipids that can prevent phagolysosome fusion, which may impact downstream MHC class II antigen processing [14,15]. Given the profound attenuation observed with loss of the LprG-Rv1410 operon in immunodeficient mice and the immunomodulatory role of LprG, we hypothesized that deletion of the LprG-Rv1410 locus may result in an improved whole cell *Mtb* vaccine.

Results

The ΔLprG vaccine protects against Mtb challenge in mice and has a comparable attenuation to BCG

We wanted to evaluate the potential use of the previously characterized H37Rv*ΔlprG-rv1410* (ΔLprG) deletion strain [11] as an alternative whole cell vaccine to BCG. We determined that ΔLprG induced Ag-specific T cells in peripheral blood of both C57BL/6J and Balb/cJ mice and tested the protective efficacy of the ΔLprG mutant as a vaccine strain in these backgrounds (Fig 1A–1F). Both ΔLprG and BCG vaccinated C57BL/6 (Fig 1A–1C) and Balb/cJ mice

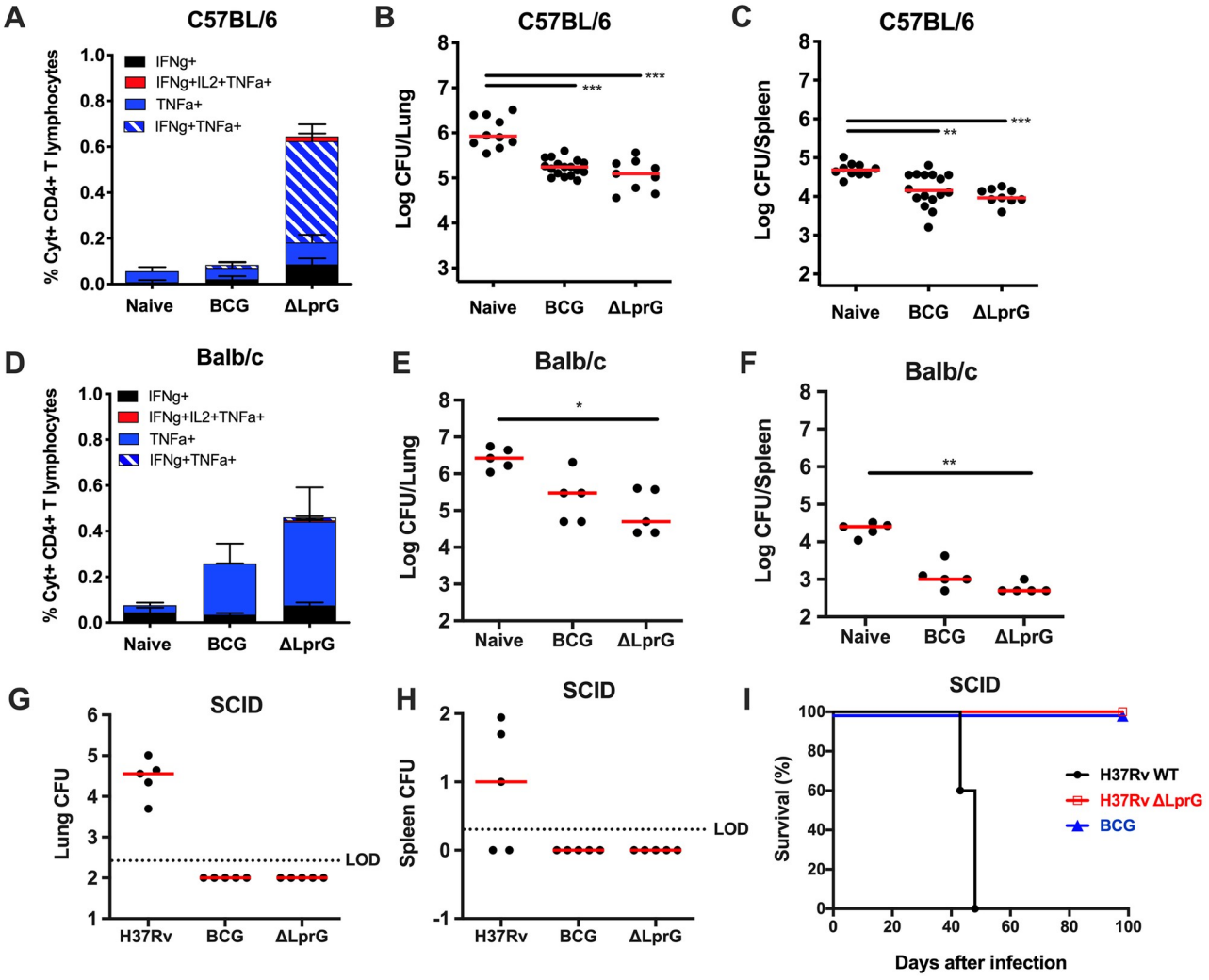

Fig 1. Protective efficacy of ΔLprG and BCG vaccines in C57BL/6J and Balb/cJ mice and attenuation in SCID mice. C57BL/6J or Balb/cJ mice were vaccinated with 100uL of O.D. 1.0 log-phase culture of either BCG Serum Statens Institute (SSI) or H37Rv*ΔlprG-rv1410c* (ΔLprG) subcutaneously in the left flank. Peripheral blood mononuclear cells (PBMC) were collected 2 weeks post-vaccination. Percent cytokine positive (%Cyt$^+$) antigen-specific T lymphocyte responses are shown as measured by intracellular cytokine staining (ICS) in CD4$^+$ CD44$^+$ T lymphocytes following stimulation with purified protein derivative (PPD, Synbiotic Tuberculin OT). Mice were aerosol-challenged with 75 CFU of *Mtb H37Rv*. Colony-forming units (CFU) were counted from lung or spleen at week 4 following challenge; C57BL/6 **(A-C) and** Balb/cJ **(D-F)** mice. SCID mice received approximately 75 CFU of aerosolized *Mtb H37Rv*, BCG SSI, or ΔLprG. CFU from lung **(G)** or spleen **(H)** of SCID mice 4 weeks post-infection. **I)** Survival curve from **(G,H)** showing survival of mice receiving aerosolized ΔLprG and BCG vaccines out to 100 days. Kruskall-Wallis with Dunn's correction for multiple comparisons; * $p<0.05$; ** $p<0.01$; *** $p<0.001$; **** $p<0.0001$. Red bar = median. Data is one representative experiment out of three with 5–15 mice per group for C57BL/6J mice. Balb/cJ and SCID challenges were performed once with 5 mice per group.

https://doi.org/10.1371/journal.ppat.1009096.g001

(Fig 1D and 1F) demonstrated immunogenicity and reduced bacterial loads as compared to non-vaccinated mice (Naïve) after *Mtb* challenge. We have previously published that the ΔLprG deletion strain was significantly attenuated in SCID mice as compared to WT and complemented mice after IV inoculation (Martinot et al., 2016). We further confirmed the attenuation phenotype with an aerosol administration of the ΔLprG vaccine in SCID mice, which showed a similar attenuation profile to BCG (Fig 1G and 1H). All BCG and ΔLprG vaccinated mice survived >100 days, whereas all *Mtb* infected mice died by day 50 (Fig 1I).

ΔLprG vaccination leads to enhanced immunogenicity and protection in mice that develop necrotizing granulomas

We were interested in studying the effect of attenuated whole cell vaccines on the structure and function of TB granulomas. We reasoned that vaccination studies in mice may fail to predict vaccine efficacy in humans in part due to the fact that common mouse models used in TB vaccine research do not recapitulate classic TB pathology observed in humans. Therefore, we tested the immunogenicity of BCG and ΔLprG vaccines in C3HeB/FeJ mice, which develop necrotizing granulomas that are similar to human TB granulomas. C3HeB/FeJ mice have a genetic susceptibility locus *sst1* that renders them highly susceptible to tuberculosis disease [16], and they develop lesions with central necrosis characterized by neutrophilic infiltrates that can develop into caseous and hypoxic lesions over time [17,18]. Furthermore, we wanted to assess vaccine immunogenicity longitudinally in peripheral blood of mice. C3HeB/FeJ mice were vaccinated by the subcutaneous route with $2x10^7$ colony-forming units (CFU) of either BCG or ΔLprG, formulated in phosphate-buffered saline with tyloxapol and glycerol [19]. Serum was collected for Luminex analysis of cytokine and chemokine responses on days 0, 1, and 7 following vaccination, and PBMC were isolated at weeks 2, 6, and 9 (Fig 2A). ΔLprG vaccination resulted in greater levels of serum inflammatory cytokines G-CSF ($p = 0.0159$), IL-6 ($p = 0.0317$), and IP-10 ($p = 0.0079$) than BCG on day 1 and day 7 ($p = 0.0159$, $p = 0.0079$, $p = 0.0079$, respectively) following vaccination (Fig 2B–2H). ΔLprG vaccination also led to greater serum MIG ($p = 0.0159$) and MCP-1 ($p = 0.0079$) than BCG on day 7 (Fig 2D and 2F).

We next evaluated Ag-specific T lymphocyte responses in peripheral blood. ESAT-6, Ag85B, and TB10.4 are thought to potentially play a role in both innate immune signaling and protective immunity to TB [3,20,21]. Ag85B and ESAT-6 specific CD4+ T lymphocytes were detected in C57BL/6J mice exposed to *Mtb* lacking the LprG-Rv1410 operon, although at significantly lower levels than those induced by virulent *Mtb*, presumably due to the lack of replication of the mutant *Mtb* as compared to wild-type H37Rv (S1 Fig). On the contrary, C3HeB/FeJ mice are H2-k restricted, and Ag85B and ESAT-6 specific responses were below the limit of detection by intracellular cytokine staining. Therefore, PBMC were stimulated with purified protein derivative (PPD; Tuberculin OT, Synbiotic) and were assessed by ICS assays. Higher IFN-γ-, TNF-α-, and IL-2-secreting $CD4^+$ T cell responses were observed in the blood of ΔLprG vaccinated mice as compared to BCG vaccinated mice at week 2 following vaccination (Fig 3A; $p = 0.004$), and these differences persisted at week 6 and week 9. In contrast, Ag-specific $CD8^+$ T cell responses were comparable between ΔLprG and BCG vaccinated mice (Fig 3B) in blood. ΔLprG mice also demonstrated increased numbers of Ag-specific CD4+ T lymphocytes in lung (Fig 3C) and spleen (Fig 3E) 2 weeks post-vaccination. Similar to blood, minimal differences were noted in lung and splenic CD8+T lymphocyte populations post-vaccination (Fig 3D and 3F).

At week 9, mice were challenged by the aerosolized route with 75 colony-forming units (CFU) of *Mtb* H37Rv and were sacrificed at week 4 following challenge to assess protective efficacy and immune correlates of protection. Prior to tissue harvest, lungs were perfused with

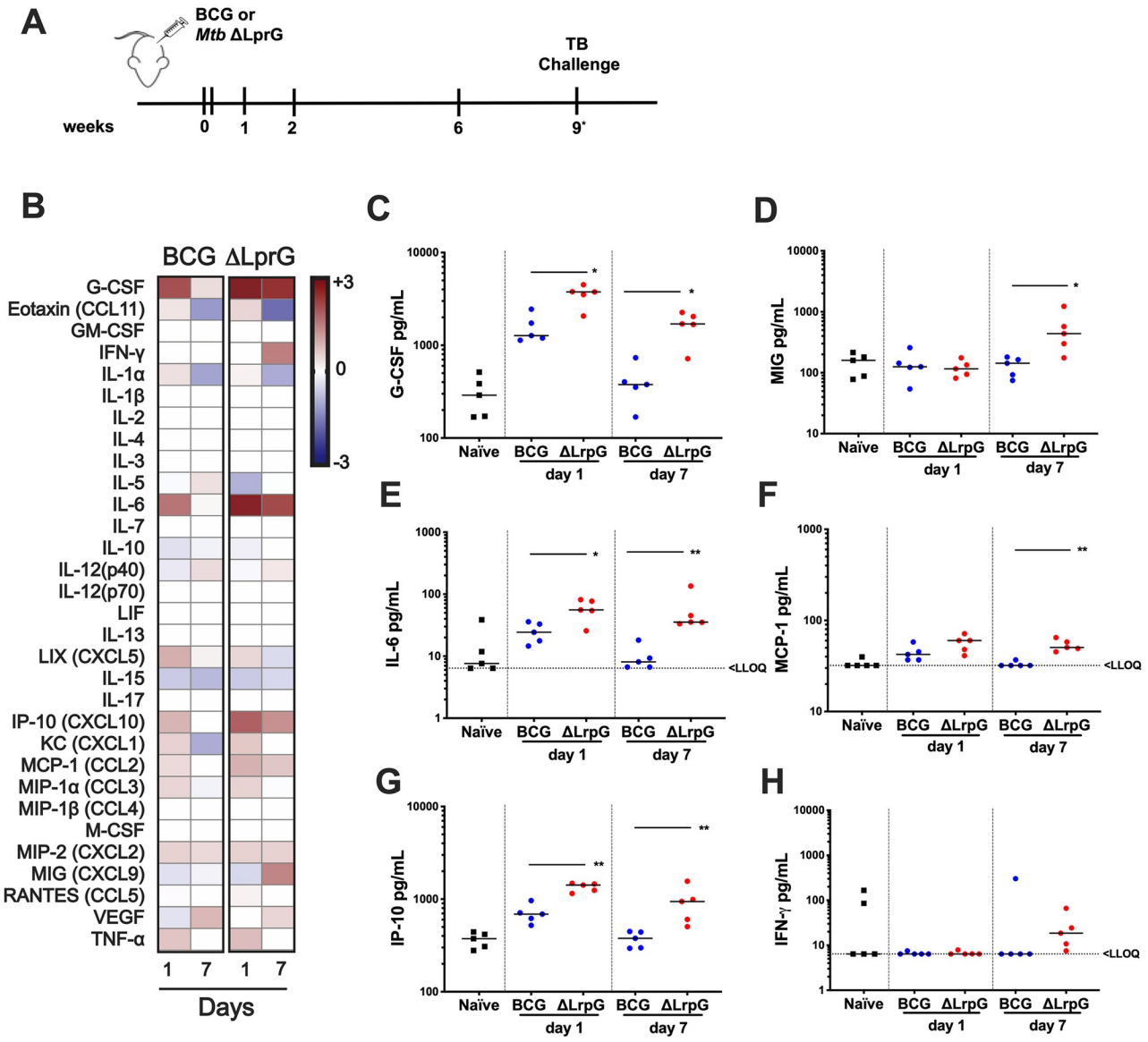

Fig 2. Induction of pro-inflammatory cytokines by ΔLprG and BCG vaccines in C3HeB/FeJ mice. A) Vaccination regimen. C3HeB/FeJ mice were vaccinated with 100uL of O.D. 1.0 log-phase culture of either BCG Serum Statens Institute (SSI) or H37RvΔ*lprG-rv1410c* (ΔLprG) subcutaneously in the left flank. Serum for Luminex cytokine analysis was collected on days 1 and 7 after vaccination. PBMC were collected at weeks 2, 6, and 9 post-vaccination. **B)** Heat-map showing median log2 fold-change of serum cytokine levels as compared to naïve mice in BCG and ΔLprG vaccinated mice on days 1 and 7. **C-H)** Individual cytokine levels in serum on days 1 and 7; bar represents median values;* $p<0.05$; ** $p<0.01$, Mann-Whitney U test (BCG vs. ΔLprG). LLOQ represents lower limit of quantification. Luminex assays were performed twice with 5–8 mice per group. Data is representative of individual experiments.

https://doi.org/10.1371/journal.ppat.1009096.g002

phosphate-buffered saline (PBS) to clear peripheral erythrocytes and leukocytes from the pulmonary vasculature. Lungs were collected and homogenized, and pulmonary T cells were purified and stimulated with PPD and analyzed by ICS assays for IFN-γ, TNF-α, IL-2, IL-17, and IL-10.

C3HeB/FeJ mice vaccinated with the ΔLprG vaccine demonstrated a median 1.3 $\log_{10}$ reduction in bacterial CFU in lung (Fig 4A) and a 1.2 median $\log_{10}$ reduction in bacterial CFU in spleen (Fig 4B) as compared with unvaccinated (Naïve) mice. Although the ΔLprG vaccine

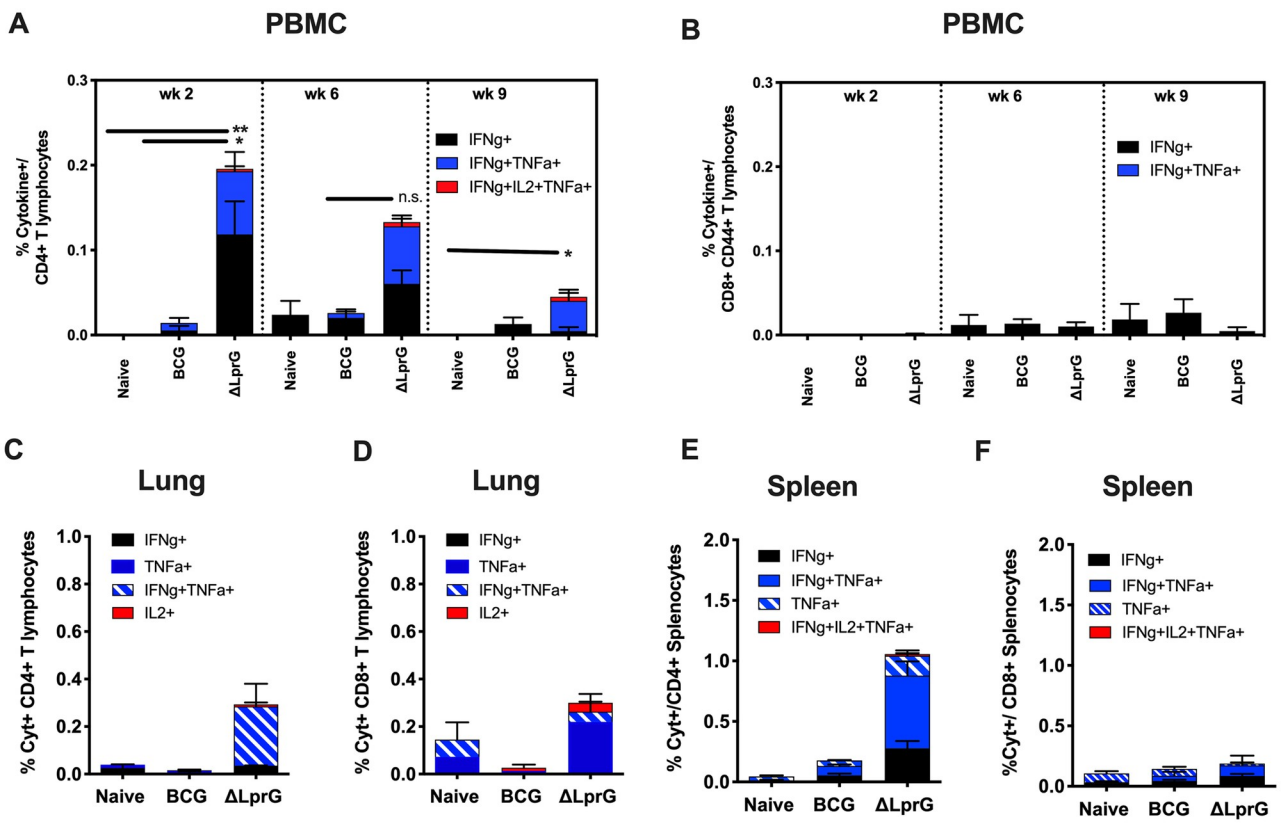

Fig 3. Immunogenecity of BCG and ΔLprG vaccines in C3HeB/FeJ mice. PBMC were collected at week 2, 6, and 9 following vaccination (**A,B**). Lung leukocytes (**C,D**) and splenocytes (**E,F**) were collected 2 weeks following vaccination. Percent cytokine positive (%Cyt$^+$) antigen-specific T lymphocyte responses as measured by intracellular cytokine staining (ICS) in CD4$^+$ (**A,C,E**) and CD8$^+$ (**B,D,F**) CD44$^+$ T lymphocytes following stimulation of PBMC, lung leukocytes, or splenocytes with purified protein derivative (PPD, Synbiotic Tuberculin OT). Percentages reflect subsets of cytokine secreting cell populations from Boolean analysis (FlowJo v10) of all possible cytokine combinations (IFNγ, TNF-α, IL-2, IL-17A, and IL-10); * $p<0.05$; ** $p<0.01$, Kruskall-Wallis for total % Cyt+ cells with Dunn's corrections for multiple comparisons. Data is representative of individual experiments. PBMC ICS was performed 4 times with 5–10 animals per vaccine group. Lung leukocytes and splenocyte analyses were performed once with 5–10 animals per group. Data presented is from two different replicates.

https://doi.org/10.1371/journal.ppat.1009096.g003

resulted in equivalent protection to BCG in C57BL/6J and Balb/cJ mice, the ΔLprG vaccine showed better protection than BCG in C3HeB/FeJ mice with a median 0.9 $\log_{10}$ greater reduction in CFU in lung (Fig 4A; $p<0.05$). BCG afforded less protection in C3HeB/FeJ mice as compared with C57BL/6J and Balb/cJ mice (Fig 1). Dose finding studies in C57BL/6J mice suggested that vaccine dose was unlikely to contribute to the improved protective efficacy seen in C3HeB/FeJ mice vaccinated with the ΔLprG vaccine, since 1 log lower vaccine dose (10^6 CFU versus 10^7 CFU) showed only minimal differences in protective efficacy for BCG or ΔLprG in C57BL/6J mice (S2 Fig).

At necropsy, ΔLprG and BCG vaccinated mice had fewer and smaller granulomas as compared to naïve mice (Fig 4C), but ΔLprG vaccinated animals had significantly fewer granulomas with acid-fast bacteria (Fig 4D), consistent with the overall decreased bacterial burden compared to lungs from BCG vaccinated and unvaccinated animals. Unvaccinated mice had multiple granulomas >1 mm^2 in area (Fig 4C and 4E) with neutrophilic infiltrates and necrosis (Fig 4E), as compared to BCG and ΔLprG vaccinated mice (Fig 4F and 4G). Pathology in non-vaccinated mice was characterized by multibacillary proliferation of acid-fast bacteria within macrophages (Fig 4H, inset), whereas ΔLprG vaccination was associated with

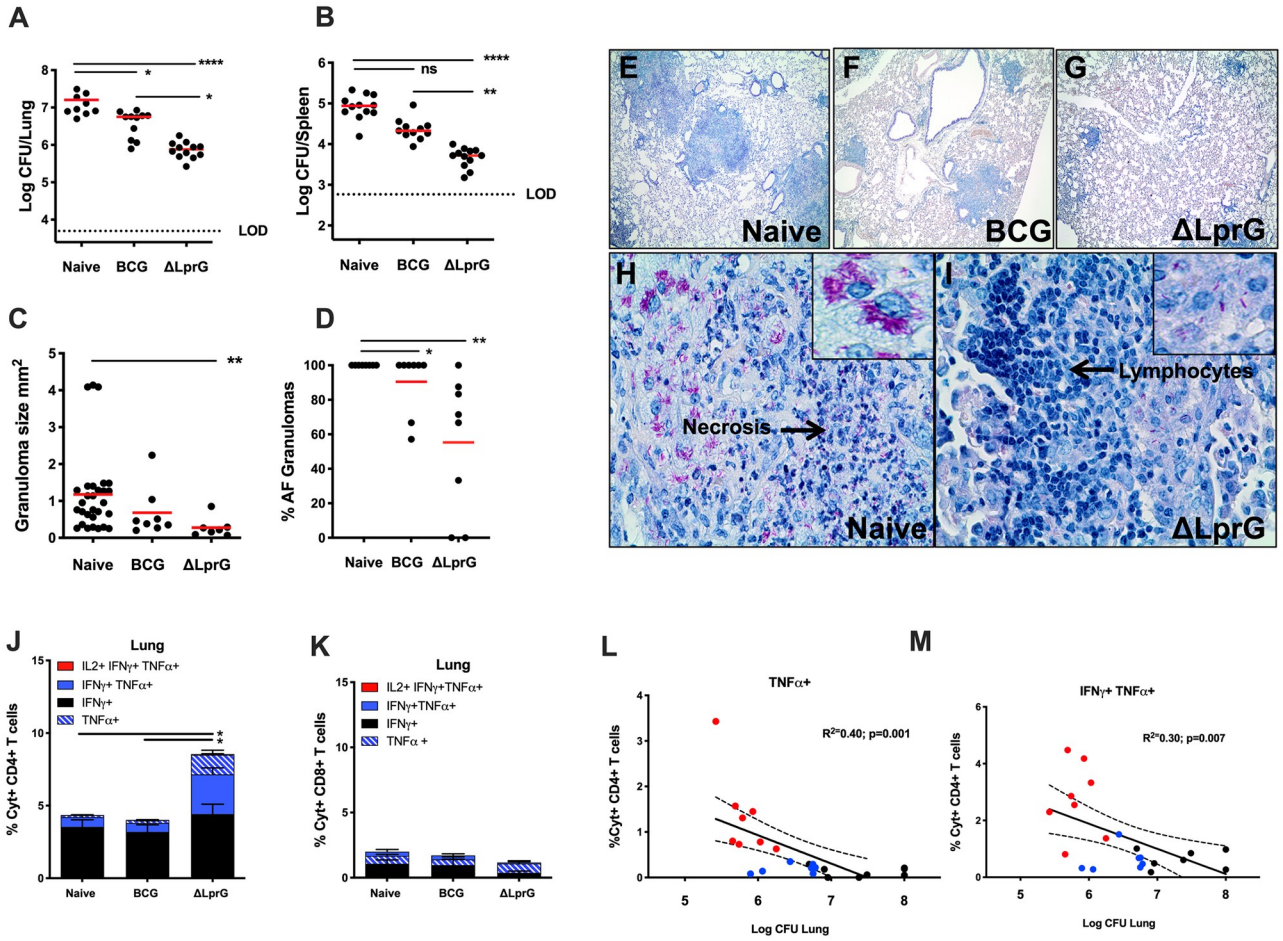

Fig 4. Protective efficacy of ΔLprG and BCG vaccines against *Mtb* challenge in C3HeB/FeJ mice. Colony-forming units (CFU) from **A)** lung or **B)** spleen at week 4 following challenge with 75 CFU of aerosolized *Mtb H37Rv*. Histopathology on lungs from naïve and vaccinated C3HeB/FeJ mice following aerosol *Mtb* challenge showing **C)** individual granuloma size (mm^2) in lungs from mice at week 4 following challenge and **D)** percent of granulomas that contain visible acid-fast organisms. Dots represent individual animals (**C**) and individual granuloma measurements (**D**). Kruskall-Wallis with Dunn's correction for multiple comparisons; * $p<0.05$; ** $p<0.01$; *** $p<0.001$; **** $p<0.0001$. Red bar = median. Representative images of Ziehl-Neelsen acid-fast staining in affected lung from **E)** Naïve **F)** BCG vaccinated and **G)** ΔLprG vaccinated mice, 4 weeks post-*Mtb* aerosol challenge, at 100x magnification. Representative images of Ziehl-Neelsen acid-fast staining in affected lung from **H)** Naïve and **I)** ΔLprG vaccinated mice, 4 weeks post-*Mtb* challenge, at 400x magnification. Percent cytokine positive (%Cyt^+) antigen-specific T lymphocyte responses as measured by intracellular cytokine staining (ICS) following stimulation with PPD (Synbiotic; Tuberculin OT) in **J)** $CD4^+$ or **K)** $CD8^+$ $CD44^+$ T lymphocytes isolated from lungs of C3HeB/FeJ mice at week 4 following aerosol *Mtb* challenge; * $p<0.05$, Kruskall-Wallis with Dunn's corrections for multiple comparisons. Pearson's correlation (R^2) of **L)** $TNF\alpha^+$ and **M)** $IFN\gamma^+$ $TNF\alpha^+$ $CD44^+$ $CD4^+$ T cells in lung post- *Mtb* challenge with Log10 CFU in lung following challenge. Protection data **(A-D)** is representative of 3 individual challenge experiments with 8–10 mice per group. Lung leukocyte levels post-challenge and CFU correlation analyses **(J-M)** are representative of 2 independent *Mtb* challenges with 8–10 mice per group. Red = ΔLprG-vaccinated; Blue = BCG-vaccinated; Black = Naïve mice.

https://doi.org/10.1371/journal.ppat.1009096.g004

formation of granulomas with few to no acid-fast bacteria surrounded by infiltrates of lymphocytes (Fig 4I, inset).

ΔLprG vaccinated mice showed greater Ag-specific $CD4^+$ T cell responses in lung than did BCG vaccinated mice and unvaccinated animals at necropsy post-*Mtb* challenge (Fig 4J; $p = 0.027$ and $p = 0.013$, respectively). In contrast, no differences were observed in Ag-specific $CD8^+$ T cell responses in lung post-challenge across groups (Fig 4K). $CD4^+$ and $CD8^+$ T cells responses in spleen post-challenge did not substantially differ between groups (S3 Fig). These data suggest that induction of $CD4^+$ T lymphocytes in lungs of ΔLprG vaccinated mice may have contributed to the improved protection in C3HeB/FeJ mice. Indeed, reduction in

bacterial CFU in lung correlated with both TNF-α- (Fig 4L; p = 0.001) and IFN-γ/TNF-α-secreting $CD4^+$ T cells in lung post-challenge (Fig 4M; p = 0.007).

ΔLprG vaccination is associated with decreased PD-1 expression on antigen specific T cells and correlates with improved bacterial control after Mtb challenge

Waning of BCG-induced immunity in humans has been reported to be associated with functionally exhausted effector T-lymphocytes [22,23]. PD-1 expression has also been linked to chronic antigenic stimulation and T cell exhaustion during *Mtb* infection [24]. We therefore assessed PD-1 expression on Ag-specific cytokine-secreting (Cyt+) $CD4^+$ T lymphocytes from lungs of mice at week 4 following *Mtb* challenge. ΔLprG vaccination resulted in higher PD-1-negative cytokine-secreting Ag-specific $CD4^+$ T cell responses in lung than did BCG vaccination or no vaccination post-challenge (Fig 5A; p = 0.002 to p = 0.006; S4 Fig). In contrast, PD-1-positive cytokine-secreting Ag-specific $CD4^+$ T cell responses in lung did not differ across groups (Fig 5B) despite variation in bacterial burden across groups (Fig 4A). Prior studies have shown that cells upregulate PD-1 as antigen-experienced cells transition from a central memory to effector state [25]. PD-1-positive cytokine-negative T lymphocytes may represent exhausted T cells [26]. ΔLprG vaccination was associated with significantly lower percentages of cytokine-negative PD-1-positive T cells in lung, reflecting reduced bacterial burden (Fig 5C) and cytokine-negative PD-1-positive $CD4^+$ T-lymphocytes in lung correlated with bacterial CFU in lung following challenge (Fig 5D; $p<0.0001$). Among cytokine-secreting Ag-specific CD4+ T cell subsets, PD-1-negative Ag-specific $CD4^+$ T cells in lung correlated with decreased bacterial burden (Fig 5E–5H), whereas PD-1-positive Ag-specific $CD4^+$ T cells in lung correlated with increased bacterial burden (Fig 5I–5L), suggesting the importance of PD-1-negative memory T cells for protection against *Mtb* [26].

ΔLprG vaccine efficacy correlates with serum IL-17A levels post-vaccination in C3Heb/FeJ mice

The efficacy of BCG has also been hypothesized to involve IL-17 secreting Ag-specific $CD4^+$ T cells (Th17) cells in lung [27,28], and expansion of Th17 cells in lung has been linked to improved vaccine-outcomes for experimental TB vaccines [29,30]. Genome-wide association studies have also linked polymorphisms in IL-17 regulatory genes to poor TB clinical outcomes in patients [31,32]. IL-17+ cells were below the limit of detection in lung and spleen pre-challenge (post-vaccination), and we therefore assessed the expansion of polyfunctional IL-17 secreting CD4+ T cells across vaccine groups following *Mtb* challenge. IL-17A-secreting Ag-specific $CD4^+$ T cell populations were increased in ΔLprG vaccinated mice post-challenge compared with naïve or BCG vaccinated mice (Fig 6A). Moreover, ΔLprG vaccinated mice demonstrated significantly higher PD-1-negative IL-17A-secreting $CD4^+$ T cells in lung compared to naïve and BCG vaccinated mice (Fig 6B, p = 0.013 and 0.020, respectively).

We then asked whether we could use serum cytokine screening to detect early induction of a Th17 cytokine signature during peak immunogenicity post-vaccination, thereby functioning as an early screen for vaccine efficacy in C3HeB/FeJ mice. Consistent with these data, serum IL-17A at week 2 following vaccination was elevated in ΔLprG vaccinated mice as compared to naïve and BCG-vaccinated mice (Fig 6C, p = 0.0053 and 0.0053, respectively). Serum IL-17A levels at week 2 following vaccination correlated with IL-17A-secreting $CD4^+$ T cells in lungs following challenge (S1 Table). Indeed, elevated IL-17A levels in serum 2 weeks post-vaccination significantly correlated with reduced lung bacterial burden 4 weeks post-*Mtb* challenge (Fig 7A; p = 0.015). IL-6, IL-1β, and IL-23 have also been reported as Th17 polarizing

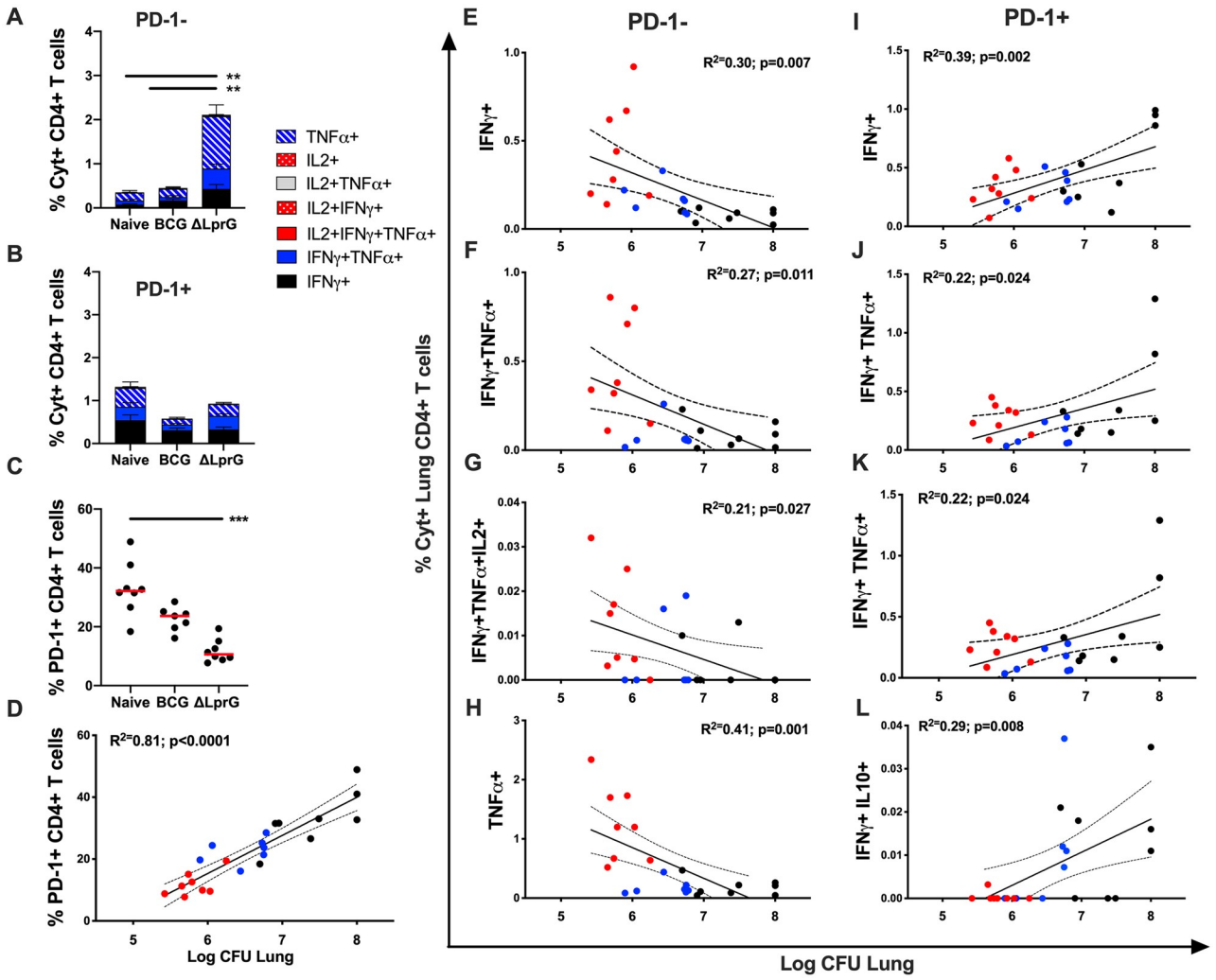

Fig 5. Cellular immune responses in C3HeB/FeJ lung post-*Mtb* challenge in BCG and ΔLprG vaccinated mice. Percent **A)** PD-1-negative (PD-1$^-$) and **B)** PD-1-positive (PD-1$^+$) cytokine-positive (Cyt$^+$) CD4$^+$ T cells in lung as measured by intracellular cytokine-staining after stimulation with PPD (Synbiotic; Tuberculin OT) from Naïve and vaccinated mice 4 weeks post-*Mtb* challenge. **C)** Percent PD-1$^+$ CD44$^+$ CD4$^+$ cytokine-negative T lymphocytes. Kruskall-Wallis with Dunn's corrections for multiple comparisons; * $p<0.05$; ** $p<0.01$; *** $p<0.001$. Red bar = Median. **D)** Pearson's correlation (R^2) of percent PD-1$^+$ cytokine-negative CD44$^+$ CD4$^+$ T lymphocytes with CFU in lung following challenge. Pearson's correlation of PD-1-Cyt$^+$ CD44$^+$ CD4$^+$ T lymphocytes **(E-H)** and PD-1$^+$ CD44$^+$ CD4$^+$ T lymphocytes **(I-L)** with CFU in lung following challenge. **(D-L)** Red = ΔLprG-vaccinated; Blue = BCG-vaccinated; Black = Naïve mice. Data representative of 2 independent experiments with 5–8 mice per group. See also S4 Fig.

https://doi.org/10.1371/journal.ppat.1009096.g005

cytokines [27]. IL-6, MIP-1α, MIP-2, and IP-10, were also elevated in BCG and ΔLprG vaccinated mice (S5 Fig) and individually correlated with decreased bacterial burden in lungs following challenge (Fig 7B–7E; p = 0.002 to p = 0.02). To determine if a combination of cytokines would be a better correlate of protection, we used a multiple linear regression analysis to develop a serum cytokine signature that included IL-17A, IL-6, MIP-1α and IP-10a, which correlated with CFU levels in both lung (p = 0.008) and in spleen (p = 0.02) following challenge (Fig 7F). However, this combined cytokine signature did not outperform individual cytokines alone, specifically IL-6 and IL-17A, in correlating with protection (S2 Table).

We next assessed the protective efficacy of the ΔLprG vaccine and the predictive capacity of serum IL-17A levels against challenge with the *Mtb* Erdman strain. In animal models such as the rabbit which demonstrate necrotizing granulomas with *Mtb* infection, Erdman is

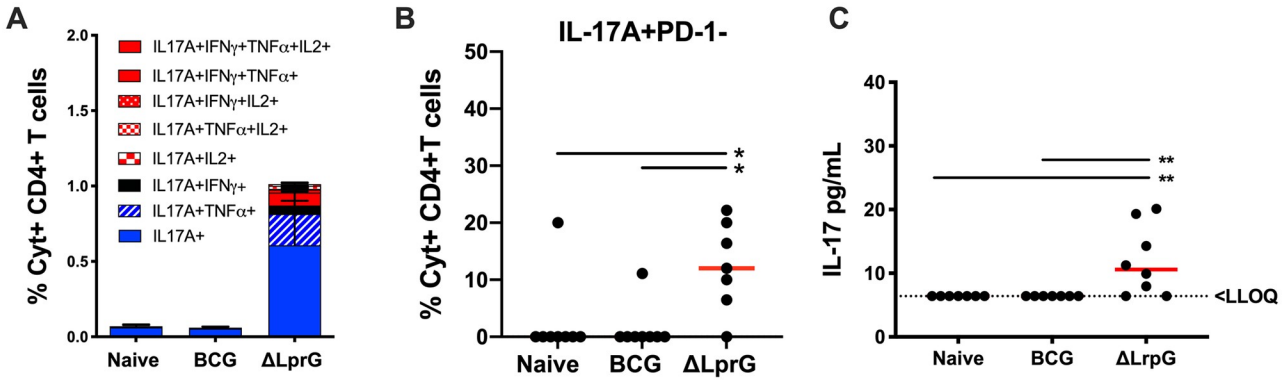

Fig 6. Lung Th17 cells and serum IL-17 induced by ΔLprG and BCG vaccines. A) Percent cytokine positive (Cyt+) Ag-specific IL-17A$^+$ CD44$^+$ CD4$^+$ T cells in lung at week 4 after *Mtb* challenge as measured by intracellular cytokine staining (ICS) post-stimulation with PPD (Synbiotic; Tuberculin OT). **B)** Percent total IL17A$^+$ PD-1$^-$ CD44$^+$ CD4$^+$ T lymphocytes in lung at week 4 following challenge. Kruskall-Wallis with Dunn's corrections for multiple comparisons; * $p<0.05$. Red bar = median. **C)** Serum IL-17 at week 2 after vaccination via Luminex. Kruskall-Wallis with Dunn's corrections for multiple comparisons;* $p<0.05$; ** $p<0.01$. Red bar = median. LLOQ = Lower Limit of Quantification. Lung leukocyte Th17 data and Luminex data representative of 2 independent experiments with 5–8 mice per group. See also S1 Table.

https://doi.org/10.1371/journal.ppat.1009096.g006

considered more pathogenic [33], and thus *Mtb* Erdman is generally considered a stringent challenge strain for vaccine studies. Furthermore, the genetic deletion of the LprG-Rv1410 operon was on the H37Rv background, and we wanted to test efficacy with a challenge strain different from that used to generate the ΔLprG vaccine. We vaccinated mice as described

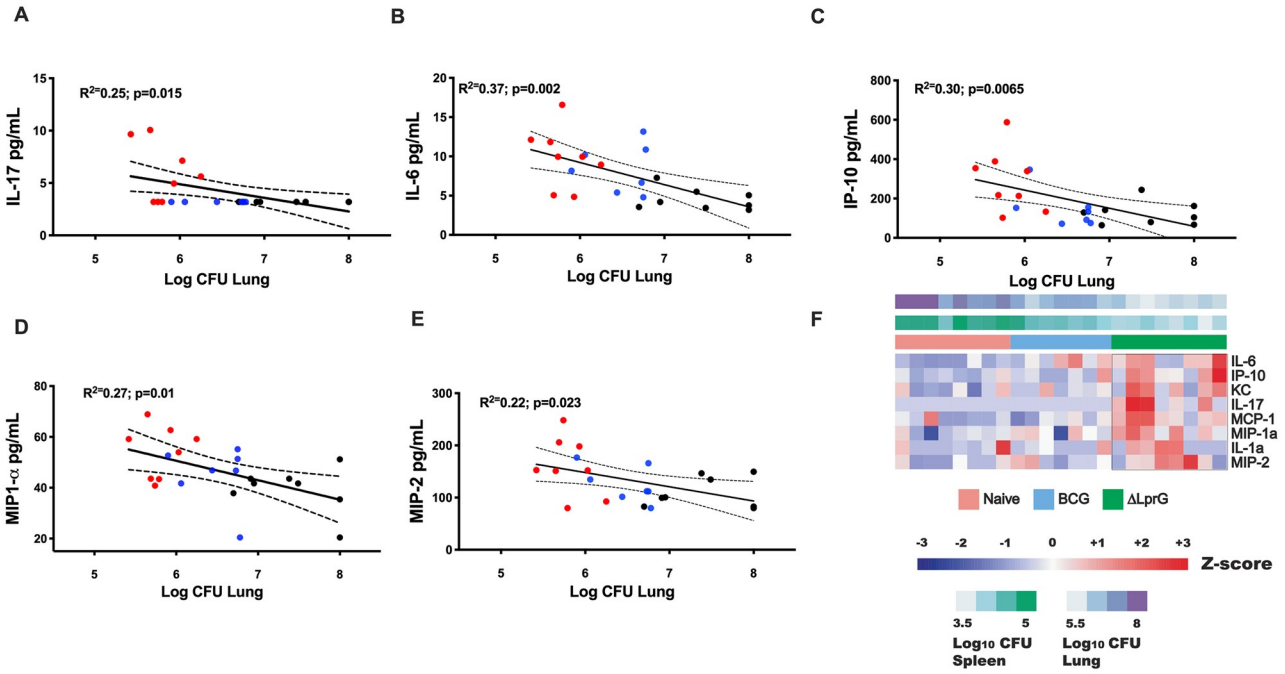

Fig 7. Correlations of serum cytokine levels following vaccination with CFU in lung following *Mtb* challenge. Serum cytokine levels from naïve and vaccinated mice were assessed at week 2 after vaccination by Luminex assays. Mice were challenged with 75 CFU *Mtb*. Pearson's correlations of cytokine levels with CFU in lung following challenge for **A)** IL-17 **B)** IL-6 **C)** IP-10 **D)** MIP1-α and **E)** MIP-2. Red = ΔLprG vaccinated; Blue = BCG vaccinated; Black = Naïve mice. **F)** Heatmap of the normalized cytokines serum levels using z-score approach, correlated with Log10 CFU in lung (purple) and spleen (green) two weeks post-vaccination in Naïve (coral), BCG (light blue), and ΔLprG (green) vaccinated mice. CFU levels were used as a continuous variable. Each column represents an individual animal and each row represents an individual cytokine. Z-score levels range from blue (negatively correlated with CFU) to red (positively correlated with CFU). Serum cytokine correlation analyses are representative of two experiments with 8–10 mice per group. See also S2 Table.

https://doi.org/10.1371/journal.ppat.1009096.g007

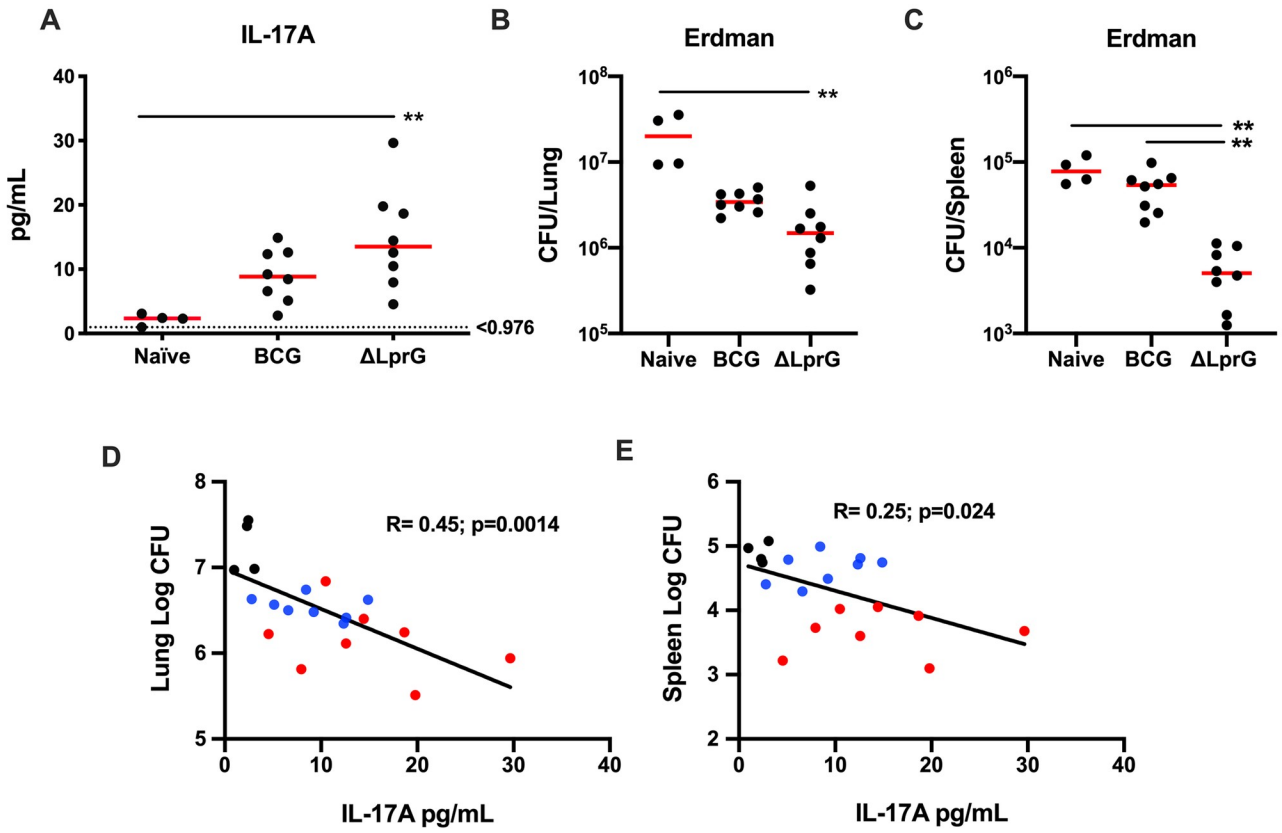

Fig 8. Validation of IL-17 serum immune correlate using high-sensitivity Luminex and *Mtb* Erdman challenge. Serum was collected from mice at week 2 following vaccination with BCG or ΔLprG as well as from naïve mice. **(A)** Serum IL-17A levels were evaluated using a high-sensitivity Luminex assay. Kruskall-Wallis with Dunn's corrections for multiple comparisons; $^{**}p<0.01$. Lower limit of quantification = 0.976 pg/mL. Red lines reflect median values. Log CFU in lung **(B)** and spleen **(C)** in C3HeB/FeJ in unvaccinated (Naïve) mice and in BCG or ΔLprG vaccinated mice at week 4 following aerosol challenge with 75 CFU *Mtb* Erdman. Pearson's correlation of lung **(D)** and spleen **(E)** Log CFU following challenge with serum IL-17A levels following vaccination. Red = ΔLprG vaccinated; Blue = BCG vaccinated; Black = Naïve mice. Validation of serum IL-17 correlation with CFU following Erdman challenge was performed once with 4–8 mice per group. See also S7 Fig.

https://doi.org/10.1371/journal.ppat.1009096.g008

above and used a high sensitivity IL-17A Luminex panel to better quantify IL-17A levels in sera at week 2 following vaccination. Mice were then challenged with the *Mtb* Erdman strain. ΔLprG and BCG vaccination led to consistent induction of serum IL-17A two weeks following vaccination (Fig 8A), but ΔLprG afforded greater protection against *Mtb* Erdman challenge with a median 1.1 log reduction in bacterial CFU in lung (Fig 8B; p = 0.001) and a median 1.2 log reduction in bacterial CFU in spleen (Fig 8C; p = 0.002) compared to unvaccinated controls. In contrast, BCG afforded only a modest reduction in CFU in lung and spleen in this stringent challenge model. Serum IL-17A levels at week 2 following vaccination inversely correlated with bacterial burden in both lung (Fig 7D, p = 0.0014) and spleen (Fig 7E, p = 0.024) with a ROC AUC between 0.97–1.0 (S6 Fig) [34]. In contrast, levels of IL-6 levels failed to correlate with protection against *Mtb* Erdman challenge (S7 Fig). These data suggest that serum IL-17A may be a useful early biomarker following vaccination to predict protective efficacy.

Discussion

The ΔLprG vaccine is a novel whole cell vaccine based on an *Mtb* strain that has been genetically engineered to delete key virulence factors and potential immune evasion genes. Vaccination with ΔLprG afforded equivalent protection to BCG in traditional vaccine testing models,

C57BL/6J and Balb/cJ mice, but showed enhanced protection compared to BCG in C3HeB/FeJ mice against both *Mtb* H37Rv and Erdman challenges. Protection was associated with PD-1-negative and Th17 $CD4^+$ T cells in lung post-*Mtb* challenge, and also correlated with serum IL-17A at week 2 following vaccination. These data support a model for pulmonary Th17 cells in TB vaccine efficacy and suggest that the improved efficacy of the ΔLprG vaccine over BCG in C3HeB/FeJ mice in these studies may be linked to higher induction of these immune subsets. Furthermore, we show that serum IL-17 early after vaccination should be explored as a possible biomarker for vaccine protective efficacy.

Prior studies of whole cell vaccines have included different versions of recombinant BCG, such as AERAS-22 [21, 35], in addition to whole cell mycobacterial vaccines based on attenuated clinical *Mtb* strains such as Mt103 [7,36–40]. Increasingly, whole cell vaccines have outperformed subunit and viral vectored vaccines in pre-clinical models [39–42].

The recent success reported for protection with intravenous (IV) BCG in non-human primates is promising and potentially could be enhanced with attenuated *Mtb* vaccines [43].

Vaccination with ΔLprG resulted in consistent reduction in bacterial burden following challenge in C57BL/6J and Balb/cJ mice and in C3HeB/FeJ mice following both H37Rv and Erdman *Mtb* challenges, suggesting that further studies are warranted to explore this strain as a candidate attenuated whole cell *Mtb* vaccine. Preclinical efficacy of MTBVAC has been reported in mice and guinea pigs [44], and MTBVAC is the first live attenuated *Mtb* whole cell vaccine to enter human clinical trials [7], demonstrating that attenuated *Mtb* can be administered safely in humans. The World Health Organization has stipulated that attenuated *Mtb* used as a vaccine must have two independent mutations [45]. Both MTBVAC and ΔLprG have stable genetic deletions in two genes, and both are non-pathogenic in immune deficient mice [11,46]. However, the two genetic deletions in the ΔLprG vaccine are in the same operon and therefore additional mutations may be needed prior to testing in humans. Future studies should explore whether the protective efficacy of the ΔLprG vaccine can be further enhanced by BCG priming [5] or by combining with other promising vaccine candidates [4]. We speculate that the protection afforded by the ΔLprG whole cell vaccine may be analogous to the robust protection observed with *Mtb* reinfection in cynomolgus macaques [6].

C3HeB/FeJ mice develop necrotizing granulomas more consistent with human tuberculous disease. Even as early as four weeks post-infection, pathology in C3HeB/FeJ mice showed divergent pathology from C57BL/6J and Balb/cJ mice with enhanced necrosis and neutrophilic infiltrates. Granulomas from ΔLprG vaccinated mice contained fewer mycobacteria than granulomas from BCG vaccinated mice suggesting that ΔLprG vaccination enhanced the restrictive nature of individual granulomas leading to overall decreased bacterial burden in the lung. C3HeB/FeJ mice are a preferred mouse model for evaluating the ability of antibiotics to penetrate the tissue microenvironment in pre-clinical TB drug development [47], and have been shown to be a robust model for testing vaccine efficacy [48], yet are infrequently used to test candidate TB vaccines. This may be due to the fact that there is variability in BCG protection dependent on strain [49]. In this study, BCG SSI failed to induce the typical 1 log of protection in C3HeB/FeJ mice as seen in C57BL/6J and Balb/cJ mice. The relatively modest protection with BCG vaccination in C3HeB/FeJ mice in our studies may have been related to the *Mtb* challenge strains used or the higher infectious inoculum (75 CFU as compared to 25 CFU) as compared with other studies [48]. Furthermore, C3HeB/FeJ mice are H2-k restricted and fail to present several $CD4^+$ T lymphocyte antigens typically studied in the context of TB vaccines such as Ag85B which can limit comparison to the existing literature. Our data supports the use of this model for evaluating candidate TB vaccines in that it provides valuable insight on the ability of vaccines to improve function and clearance of bacteria at the level of the granuloma.

Future studies should evaluate the efficacy of ΔLprG and other candidate vaccines in long-term protection studies in C3HeB/FeJ mice. Emerging data have shown the conservation of immunodominant T cell epitopes across *Mtb* strains and the potential negative impact of immunodominant T cell responses on vaccine efficacy [50–52]. It will therefore be important to test candidate TB vaccines in multiple mouse models, including those that limit expansion of immunodominant clones to traditional TB antigens. Use of H2-k restricted mice such as C3HeB/FeJ may potentially enhance the identification of important subdominant antigen-specific responses induced by whole cell vaccines.

Vaccination with ΔLprG resulted in polyfunctional polyclonal Ag-specific $CD4^+$ T cells to a PPD antigen, which included Th17 cells that co-expressed IFN-γ, TNF-α, and IL-2, key cytokines that have been reported to contribute to control of *Mtb* [53–56]. However, numerous studies in humans have shown that induction of polyfunctional $CD4^+$ T cells in peripheral blood and lung are insufficient to predict efficacy of candidate TB vaccines [57]. Although relatively small, higher percentages of Ag-specific IL-17A expressing T cell subpopulations were seen in lungs of ΔLprG vaccinated mice post-*Mtb* challenge. Interestingly, induction of Th17 subsets was low in BCG vaccinated C3HeB/FeJ mice post-challenge, and BCG protection in C3HeB/FeJ mice was lower in these studies as compared to other published work [28], which may reflect differences in BCG vaccine preparation or strain. Future work using prime-boost regimens may enhance our ability to assess in greater detail Th17 cells post-vaccination and the potential mechanistic role of IL-17 and vaccine-elicited Th17 cells in pulmonary control of *Mtb*.

TB infection in mice, as in other chronic diseases and cancer [58], has been shown to induce T cell exhaustion that is associated with high bacterial burden in lung parenchyma [59,60]. Moreover, the diminished efficacy of BCG in adult populations has been hypothesized to reflect the generation of persistent effector memory T cells that become functionally exhausted over time [23]. In the HIV vaccine field, variation in the exhaustion profiles of candidate vaccines can have significant downstream immunological effects that could impact vaccine efficacy [61]. Although PD-1 expression was low on antigen-specific T lymphocytes in PBMC post-vaccination in C3HeB/FeJ mice, we observed strong association of PD-1-negative Ag-specific $CD4^+$ T cells with decreased bacterial burden in lungs of ΔLprG vaccinated mice *post* Mtb challenge. In contrast, PD-1-positive $CD4^+$ T cells, cytokine and non-cytokine producing cells in lung post-challenge correlated inversely with protective efficacy. Interestingly, vaccinated C3HeB/FeJ mice had increased percentages of PD-1 negative Ag-specific CD4+ T lymphocyte responses in the lung post-*Mtb* challenge. Future work will be needed to assess total cell numbers in vaccinated animals. However, these data suggest that functional, non-exhausted $CD4^+$ T cells may be critical for vaccine protection and that exhausted $CD4^+$ T cells may have a detrimental effect.

We also observed that serum IL-17A levels induced shortly after vaccination correlated with protection in C3HeB/FeJ mice. IL-17 secretion has been linked to both gamma-delta T cells and ILC3 cells, both of which have been implicated in IL-17 mediated down-stream improvements in phagocytic capacity and antigen presentation [62,63]. At early timepoints post-vaccination, ΔLprG was shown to induce numerous cytokines and chemokines associated with monocyte recruitment and activation (IP-10, MIG, and MCP-1). Correlations of serum IL-17A and associated chemokines with bacterial burden may reflect the multifactorial role of IL-17 in modulating both innate and adaptive immune responses. Future studies should explore the mechanistic role of IL-17 in vaccine responses and protection, including the use of blocking antibodies or knock-out mice, as well as correlations with lung Th17 cells prior to challenge and the generalizability of the utility of IL-17 as a serum biomarker for vaccine protective efficacy.

In summary, vaccination with ΔLprG resulted in bacterial control in lung and spleen following *Mtb* H37Rv challenge in C57BL/6J, Balb/cJ, and C3HeB/FeJ mice and also provided protection with *Mtb* Erdman challenge in C3HeB/FeJ mice. Protection was significantly associated with the percentages of PD-1-negative Th1 and Th17 Ag-specific cell populations in the lungs of mice after challenge [27,64]. Moreover, serum IL-17A levels at week 2 following vaccination correlated with protective efficacy. Taken together, these data define key immunologic pathways that may contribute to protection against *Mtb* challenges in mice. Further evaluation of the ΔLprG vaccine and the use of IL-17 as a serum biomarker for vaccine protective efficacy is warranted.

Materials and methods

Ethics statement

All animal experiments were performed under an animal protocol approved by the Harvard University Institutional Animal Care and Use and Committee.

Mice, immunizations, and *Mycobacterium tuberculosis* infections

Female 6–10-wk-old C57BL/6J, Balb/cJ, SCID, and C3HeB/FeJ (The Jackson Laboratory, Bar Harbor, ME) were housed under sterile conditions in an ABSL3 facility. Mycobacterial strains were grown in 7H9 with 10% (vol/vol) OADC (Middlebrook), 0.2% glycerol and Tween 80 and maintained at 37˚C with shaking at 100rpm unless otherwise indicated. Mycobacterial strains for vaccines lots were prepared as previously described with minor modifications [19]. Cultures of Bacillus Calmette-Guérin (BCG)-Danish (BCG SSI) originally obtained from Statens Serum Institute (Copenhagen, Denmark, *gift from William R. Jacobs)* and *Mtb* H37Rv Δ*lprG-rv1410c* (ΔLprG; *Martinot et. al. 2016*) vaccines were expanded in 7H9 with 10% OADC, 0.5% glycerol, and 0.05% Tyloxapol to a 100mL volume in roller bottles. Log phase cultures were pelleted by centrifugation at 2000 rcf for 15 min and washed with equal volume (1:1) of PBS with 0.05% Tyloxapol, re-centrifuged followed by wash with 50% volume (1:2) of PBS-0.05% Tyloxapol, then re-centrifuged and resuspended in 25% volume (1:4) of PBS-0.05% Tyloxapol with 15% glycerol. To remove clumps, 10 mL volumes of bacterial suspension were filtered twice, first through 40μm then 20μm vacuum filter units (Millipore). The optical density 600 (OD600) of a 1:10 dilution of the resultant suspension was measured and then the filtrate was back diluted to OD 1.0 or OD 5.0 with additional of PBS-0.05% Tyloxapol with 15% glycerol. Mice received immunizations of 100uL of OD 1.0 bacterial culture (2 +/- $1x10^7$ CFU/mL) in PBS-0.05% Tyloxapol with 15% glycerol subcutaneously in the left flank of either BCG SSI or ΔLprG. Some mice received H37Rv prepared in a similar fashion as a control for immunogenicity studies. For dose finding experiments, C57BL/6J mice were vaccinated with BCG Pasteur or ΔLprG from freshly propagated vaccine cultures. Mice were rested a minimum of 8 weeks post-vaccination prior to aerosol challenge with 75 +/-25 CFU of either *Mycobacterium tuberculosis* H37Rv or Erdman.

Tissue processing and CFU enumeration

In all studies, lungs from *Mtb* challenged mice were aseptically collected 4 weeks following *Mtb* challenge and perfused with PBS prior to tissue harvest to remove red blood cells by transection of the abdominal aorta followed by injection of the right ventricle with 10mL cold sterile phosphate buffered saline. The three right lung lobes were used to enumerate CFU and were homogenized in sterile 1xPBS, followed by serial dilutions onto 7H10 plates and incubated for 3 weeks at 37˚C. The left lung lobe was collected into RPMI with 10% fetal bovine

serum (FBS) and homogenized using scissors for lung leukocyte isolation. Lung homogenate was incubated for 30 min in digestion buffer containing RPMI, FBS, Type IV collagenase (Sigma C5138) and DNase at 37˚C with gentle rocking. Lung digests were filtered through 30μm MACS SmartStrainers (Miltenyi Biotec) and washed with fresh media and resuspended in a standardized volume of 6 mL media prior to plating in 96 well U-bottom plates at an approximate density of $2x10^6$ cells per well. In some cases, the accessory lobe was inflated with 100uL of 10% neutral buffered formalin for histopathology.

Flow cytometry and intracellular cytokine staining (ICS)

Lymphocytes were isolated from either blood, spleen, or lung, stained, and analyzed by flow cytometry as previously described [65]. Antibodies (Ab) to CD8a (53–6.7), CD4 (RM4-5), CD44 (IM7), PD-1 (RMPI-30), IFN-γ (XMG1.2), TNF-α (MP6-XT22), IL-2 (JES6-5H4), IL-17 (TC11-18H10), and IL-10 (JES5-16E3) were purchased from BD Biosciences (Myrtle, U.K.), eBioscience, or BioLegend (San Diego, CA). Cell viability was assessed by LIVE/DEAD Fixable Aqua (Life Technologies). Ag-specific cells were estimated by intracellular cytokine staining (ICS). Peripheral blood mononuclear cells (PBMC), splenocytes, or lung leukocytes were stimulated with a 1:200 dilution of purified protein derivative (PPD, Tuberculin OT, Synbiotics, Corp, San Diego) and incubated for 40 min at 37˚C. After this incubation, Golgi-Plug and Golgi-Stop (BD Biosciences) were added and samples incubated for an additional 6.5 hours at 37˚C. Cells were subsequently washed and stained for surface antibody markers, then permeabilized with Cytofix/Cytoperm (BD Biosciences) and stained for intracellular cytokines. Cells were acquired on an LSR II flow cytometer (BD Biosciences). Data were analyzed using FlowJo v10.

Luminex assays for cytokine secretion

Serum samples were collected at days 1, 8 (+/- 1 day), and 14 days (+/- 1 day) post vaccination and compared to non-vaccinated Naïve mice. Samples were filtered twice through 0.2 micron 96 well filtration plates by centrifugation (Millipore), treated with 0.05% Tween-20, and assayed using a Luminex bead-based multiplex ELISA (MILLIPLEX MAP Mouse Cytokine/Chemokine Magnetic Bead Panel (Millipore; MCYTMAG-70K-PX32) according to manufacturer's instructions. Samples were fixed with 4% formaldehyde and subsequently washed prior to acquisition. Sample data were acquired on a MAGPIX instrument running xPONENT 4.2 software (Luminex Corp.) and analyzed using a five-parameter logistic model with an 80–120% standard acceptance range. The MILLIPLEX MAP Mouse High Sensitivity T cell panel (Millipore; MHSTCMAG-70K) was used to evaluate low levels of IL-17A. <LLOQ indicates lower limit of quantification for assay; extrapolated values below the LLOQ were evaluated at the LLOQ. Multiple regression analyses of cytokines serum levels with CFU in lung and spleen were performed using the R mixOmics package [66]. Heatmaps of serum cytokine and chemokine levels in lung and spleen were generated using R heatmap package.

Histopathology and image analysis

Lungs from infected mice were inflated with 10% neutral buffered formalin, processed, embedded in paraffin, and sectioned for staining. Formalin-fixed paraffin embedded (FFPE) serial tissue sections were stained with hematoxylin and eosin (H&E) and Ziehl-Neelsen acid-fast stains. Scoring for percent lung affected and acid-fast staining per granuloma was performed by two independent veterinary pathologists. Slides were digitized and lung granuloma area (mm^2) quantified using Aperio Imagescope (Leica Biosystems).

Statistical analysis

Statistical analyses were performed using Prism 8.0 (GraphPad Software). Data were analyzed by the Kruskal–Wallis test with Dunn multiple comparison post-test (more than two groups) or the two-tailed Mann–Whitney U test (for two groups). Longitudinally acquired Luminex data were analyzed using a two-tailed Mann-Whitney U test for each time point; not corrected for multiple comparisons across time points. Receiver operator curves (ROC) were generated using the ROC to baseline method with IL-17 values from the ultrasensitive Luminex assay [34].

Supporting information

S1 Fig. Effect of LprG-Rv1410 mutation on host recognition of T cell epitopes. C57BL/6J mice were injected subcutaneously with two doses of 100uL OD600 = 1.0 stocks of either BCG, *H37Rv*::*Δrv1411c-rv1410c*, or *H37Rv* and splenocytes were harvested 9 days post-boost. Percent cytokine positive $CD4^+$ and $CD8^+$ $CD44^+$ antigen-specific splenocytes as measured by intracellular cytokine staining (ICS) following stimulation with 15-mer overlapping peptide pools spanning the entire Ag85B, ESAT-6, and TB10.4 proteins. Percentages reflect subsets of cytokine secreting cell populations from Boolean analysis (FlowJo v10) of all possible cytokine combinations (IFNγ, TNF-α, IL-2, IL-17A, and IL-10). Data representative of a single experiment with 5–8 animals per group.
(TIF)

S2 Fig. Dose titration and protective efficacy of BCG Pasteur and ΔLprG vaccines in C57BL/6J mice. Female 6–8 wk old C57BL/6J mice were immunized subcutaneously with either $1x10^6$ or $1x10^7$ of freshly propagated vaccine cultures 8 weeks prior to aerosol challenge with 75 CFU of H37Rv *Mtb*. Lungs were homogenized and CFU enumerated 4 weeks post-challenge after growth on Middlebrook 7H10 agar. Data represents a single experiment performed once with 5 mice per group.
(TIF)

S3 Fig. Cytokine secretion in splenocytes from naïve and vaccinated mice following *Mtb* challenge. Naïve, BCG, or ΔLprG vaccinated mice were challenged with 75 CFU *Mtb* H37Rv. Splenocytes were collected and stimulated with PPD. Percent cytokine secreting **(A)** $CD4^+$ and **(B)** $CD8^+$ $CD44^+$ T cells are shown. Data representative of one of two experimental replicates with 5 mice per group.
(TIF)

S4 Fig. PD-1-negative $CD4^+$ T cell responses in naïve and vaccinated C3HeB/FeJ mice following *Mtb* challenge. Naïve, BCG, or ΔLprG vaccinated mice were challenged with 75 CFU *Mtb* H37Rv. T cells from lung were collected and stimulated with PPD. PD-1-negative populations shown in each panel. % IFN-γ, TNF-α, IL-2 positive $PD\text{-}1^-$ $CD4^+$ T cells are shown. Kruskall-Wallis with Dunn's corrections for multiple comparisons;* $p<0.05$; ** $p<0.01$; *** $p<0.001$. Red bar indicates median values. Data representative of 2 experimental replicates with 5–8 mice per group.
(TIF)

S5 Fig. Serum cytokine secretion in naïve and vaccinated mice at week 2 following vaccination. A) Heatmap of median log2 fold-change cytokine and chemokine secretion in sera from BCG and ΔLprG vaccinated mice as compared to naïve animals at week 2 following vaccination as measured by Luminex assays. **B-E)** Serum cytokine levels from naïve and vaccinated mice. Bars represent median values. LLOQ represents lower limit of quantification. Data

representative of two experimental replicates with 5 mice per group.
(TIF)

S6 Fig. ROC curve for high-sensitivity IL-17A serum Luminex assay. Mice were vaccinated with BCG and ΔLprG as described and sera collected for Luminex. The x-axis represents baseline percentiles and the y-axis is the probability that the BCG vaccinated values (filled squares) or ΔLprG vaccinated values (filled circles) were greater than or equal to the baseline percentile threshold as calculated using Graphpad prism v8. Data presents a single experiment performed once with 4–8 mice per group.
(TIF)

S7 Fig. Serum IL-6 levels in vaccinated mice challenged with *Mtb* Erdman. IL-6 cytokine levels in sera from BCG and ΔLprG vaccinated mice as compared to naïve animals at week 2 following vaccination as measured by Luminex assays. Correlations of serum IL-6 levels lung and spleen CFU in mice challenged with *Mtb* Erdman four weeks post-challenge. *Mtb* Erdman challenge was performed once with 4–8 mice per group.
(TIF)

S1 Table. Correlations of %IL-17A+ CD4+ T cells in lung with post-vaccination serum IL-17A levels and lung bacterial burden. Naïve, BCG, or ΔLprG vaccinated mice were challenged with 75 CFU *Mtb* H37Rv. Serum cytokine levels from naïve and vaccinated mice were assessed at week 2 after vaccination by Luminex assays. Mice were challenged with 75 CFU *Mtb* H37Rv. Mice were sacrificed at week 4 following challenge and perfused with sterile saline prior to tissue harvest. T cells in lung were collected and stimulated with PPD. Pearson's correlations of % cytokine$^+$ CD4$^+$ T cells with serum IL-17A levels following vaccination and with CFU in lung are shown, and p-values.
(EPS)

S2 Table. Correlations of serum cytokine levels following vaccination with CFU following challenge. P values of correlations of serum cytokine and chemokine levels at week 2 following vaccination with CFU levels in lung and spleen following challenge.
(EPS)

Acknowledgments

The authors thank Joern Schmitz, William Jacobs, Jaimie Sixsmith, Alex Badamchi-Zadeh, Peter Abbink, Anthony Cadena, Roderick Bronson, and Erica Borducchi for generous advice, assistance, and reagents.

Author Contributions

Conceptualization: Amanda J. Martinot, Kevin B. Urdahl, Eric J. Rubin, Dan H. Barouch.

Data curation: Amanda J. Martinot, Eryn Blass, Malika Aid.

Formal analysis: Amanda J. Martinot, Eryn Blass, Malika Aid, Anne Devorak.

Funding acquisition: Amanda J. Martinot, Kevin B. Urdahl, Dan H. Barouch.

Investigation: Amanda J. Martinot, Eryn Blass, Jingyou Yu, Shant H. Mahrokhian, Sara B. Cohen, Courtney R. Plumlee, Rafael A. Larocca, Noman Siddiqi, Shoko Wakabayashi, Michelle Gardner, Rebecca Audette.

Methodology: Amanda J. Martinot, Eryn Blass, Dan H. Barouch.

Resources: Eric J. Rubin, Dan H. Barouch.

Software: Dan H. Barouch.

Supervision: Amanda J. Martinot, Noman Siddiqi, Dan H. Barouch.

Writing – original draft: Amanda J. Martinot.

Writing – review & editing: Amanda J. Martinot, Eryn Blass, Malika Aid, Kevin B. Urdahl, Eric J. Rubin, Dan H. Barouch.

References

1. Trunz BB, Fine P, Dye C. Effect of BCG vaccination on childhood tuberculous meningitis and miliary tuberculosis worldwide: a meta-analysis and assessment of cost-effectiveness. Lancet. 2006; 367:1173–1180. https://doi.org/10.1016/S0140-6736(06)68507-3 PMID: 16616560
2. Gagneux S. Strain variation in the Mycobacterium tuberculosis complex: its role in biology, epidemiology and control. 2017.
3. Aguilo N, Gonzalo-Asensio J, Alvarez-Arguedas S, Marinova D, Gomez AB, Uranga S, et al. Reactogenicity to major tuberculosis antigens absent in BCG is linked to improved protection against Mycobacterium tuberculosis. Nature Communications. Nature Publishing Group; 2017; 8:16085. https://doi.org/10.1038/ncomms16085 PMID: 28706226
4. Van Der Meeren O, Hatherill M, Nduba V, Wilkinson RJ, Muyoyeta M, Van Brakel E, et al. Phase 2b Controlled Trial of M72/AS01E Vaccine to Prevent Tuberculosis. N Engl J Med. 2018; 379:1621–1634. https://doi.org/10.1056/NEJMoa1803484 PMID: 30280651
5. Nemes E, Geldenhuys H, Rozot V, Rutkowski KT, Ratangee F, Bilek N, et al. Prevention of M. tuberculosis Infection with H4:IC31 Vaccine or BCG Revaccination. N Engl J Med. 2018; 379:138–149. https://doi.org/10.1056/NEJMoa1714021 PMID: 29996082
6. Cadena AM, Hopkins FF, Maiello P, Carey AF, Wong EA, Martin CJ, et al. Concurrent infection with Mycobacterium tuberculosis confers robust protection against secondary infection in macaques. Salgame P, editor. PLoS Pathog. Public Library of Science; 2018; 14:e1007305. https://doi.org/10.1371/journal.ppat.1007305 PMID: 30312351
7. Tameris M, Mearns H, Penn-Nicholson A, Gregg Y, Bilek N, Mabwe S, et al. Live-attenuated Mycobacterium tuberculosis vaccine MTBVAC versus BCG in adults and neonates: a randomised controlled, double-blind dose-escalation trial. Lancet Respir Med. 2019. https://doi.org/10.1016/S2213-2600(19)30251-6 PMID: 31416768
8. Kieser KJ, Rubin EJ. How sisters grow apart: mycobacterial growth and division. Nat Rev Micro. 2014; 12:550–562. https://doi.org/10.1038/nrmicro3299 PMID: 24998739
9. Dulberger CL, Rubin EJ, Boutte CC. The mycobacterial cell envelope—a moving target. Nat Rev Micro. 2019; 159:1497. https://doi.org/10.1038/s41579-019-0273-7 PMID: 31728063
10. Farrow MF, Rubin EJ. Function of a mycobacterial major facilitator superfamily pump requires a membrane-associated lipoprotein. J Bacteriol. 2008; 190:1783–1791. https://doi.org/10.1128/JB.01046-07 PMID: 18156250
11. Martinot AJ, Farrow M, Bai L, Layre E, Cheng T-Y, Tsai JH, et al. Mycobacterial Metabolic Syndrome: LprG and Rv1410 Regulate Triacylglyceride Levels, Growth Rate and Virulence in Mycobacterium tuberculosis. PLoS Pathog. 2016; 12:e1005351. https://doi.org/10.1371/journal.ppat.1005351 PMID: 26751071
12. Drage MG, Tsai H-C, Pecora ND, Cheng T-Y, Arida AR, Shukla S, et al. Mycobacterium tuberculosis lipoprotein LprG (Rv1411c) binds triacylated glycolipid agonists of Toll-like receptor 2. Nat Struct Mol Biol. 2010; 17:1088–1095. https://doi.org/10.1038/nsmb.1869 PMID: 20694006
13. Harding CV, Boom WH. Regulation of antigen presentation by Mycobacterium tuberculosis: a role for Toll-like receptors. Nat Rev Micro. 2010; 8:296–307. https://doi.org/10.1038/nrmicro2321 PMID: 20234378
14. Shukla S, Richardson ET, Athman JJ, Shi L, Wearsch PA, McDonald D, et al. Mycobacterium tuberculosis Lipoprotein LprG Binds Lipoarabinomannan and Determines Its Cell Envelope Localization to Control Phagolysosomal Fusion. Lewinsohn DM, editor. PLoS Pathog. 2014; 10:e1004471. https://doi.org/10.1371/journal.ppat.1004471 PMID: 25356793
15. Gaur RL, Ren K, Blumenthal A, Bhamidi S, Gibbs S, Jackson M, et al. LprG-Mediated Surface Expression of Lipoarabinomannan Is Essential for Virulence of Mycobacterium tuberculosis. Behr MA, editor. PLoS Pathog. 2014; 10:e1004376. https://doi.org/10.1371/journal.ppat.1004376 PMID: 25232742

16. Pan H, Yan B-S, Rojas M, Shebzukhov YV, Zhou H, Kobzik L, et al. Ipr1 gene mediates innate immunity to tuberculosis. Nature. 2005; 434:767–772. https://doi.org/10.1038/nature03419 PMID: 15815631

17. Irwin SM, Driver E, Lyon E, Schrupp C, Ryan G, Gonzalez-Juarrero M, et al. Presence of multiple lesion types with vastly different microenvironments in C3HeB/FeJ mice following aerosol infection with Mycobacterium tuberculosis. Dis Model Mech. 2015; 8:591–602. https://doi.org/10.1242/dmm.019570 PMID: 26035867

18. Harper J, Skerry C, Davis SL, Tasneen R, Weir M, Kramnik I, et al. Mouse model of necrotic tuberculosis granulomas develops hypoxic lesions. J INFECT DIS. 33rd ed. 2012; 205:595–602. https://doi.org/10.1093/infdis/jir786 PMID: 22198962

19. Hart BE, Asrican R, Lim S-Y, Sixsmith JD, Lukose R, Souther SJR, et al. Stable Expression of Lentiviral Antigens by Quality-Controlled Recombinant Mycobacterium bovis BCG Vectors. Plotkin SA, editor. Clinical and Vaccine Immunology. 2015; 22:726–741. https://doi.org/10.1128/CVI.00075-15 PMID: 25924766

20. Hoang T, Aagaard C, Dietrich J, Cassidy JP, Dolganov G, Schoolnik GK, et al. ESAT-6 (EsxA) and TB10.4 (EsxH) based vaccines for pre- and post-exposure tuberculosis vaccination. Izzo AA, editor. PLoS ONE. Public Library of Science; 2013; 8:e80579. https://doi.org/10.1371/journal.pone.0080579 PMID: 24349004

21. Gröschel MI, Sayes F, Shin SJ, Frigui W, Pawlik A, Orgeur M, et al. Recombinant BCG Expressing ESX-1 of Mycobacterium marinum Combines Low Virulence with Cytosolic Immune Signaling and Improved TB Protection. Cell Rep. 2017; 18:2752–2765. https://doi.org/10.1016/j.celrep.2017.02.057 PMID: 28297677

22. Orme IM. Tuberculosis. Tuberculosis (Edinb). Elsevier Ltd; 2010; 90:329–332. https://doi.org/10.1016/j.tube.2010.06.002 PMID: 20659816

23. Andersen P, Woodworth JS. Tuberculosis vaccines—rethinking the current paradigm. Trends Immunol. 2014; 35:387–395. https://doi.org/10.1016/j.it.2014.04.006 PMID: 24875637

24. Jayaraman P, Jacques MK, Zhu C, Steblenko KM, Stowell BL, Madi A, et al. TIM3 Mediates T Cell Exhaustion during Mycobacterium tuberculosis Infection. PLoS Pathog. 2016; 12:e1005490. https://doi.org/10.1371/journal.ppat.1005490 PMID: 26967901

25. Crawford A, Angelosanto JM, Kao C, Doering TA, Odorizzi PM, Barnett BE, et al. Molecular and transcriptional basis of $CD4^+$ T cell dysfunction during chronic infection. Immunity. 2014; 40:289–302. https://doi.org/10.1016/j.immuni.2014.01.005 PMID: 24530057

26. Wherry EJ, Kurachi M. Molecular and cellular insights into T cell exhaustion. Nat Rev Immunol. 2015; 15:486–499. https://doi.org/10.1038/nri3862 PMID: 26205583

27. Khader SA, Bell GK, Pearl JE, Fountain JJ, Rangel-Moreno J, Cilley GE, et al. IL-23 and IL-17 in the establishment of protective pulmonary CD4+ T cell responses after vaccination and during Mycobacterium tuberculosis challenge. Nat Immunol. 2007; 8:369–377. https://doi.org/10.1038/ni1449 PMID: 17351619

28. Gopal R, Lin Y, Obermajer N, Slight S, Nuthalapati N, Ahmed M, et al. IL-23-dependent IL-17 drives Th1-cell responses following Mycobacterium bovis BCG vaccination. Eur J Immunol. 2012; 42:364–373. https://doi.org/10.1002/eji.201141569 PMID: 22101830

29. Moliva JI, Hossfeld AP, Sidiki S, Canan CH, Dwivedi V, Beamer G, et al. Selective delipidation of Mycobacterium bovis BCG enables direct pulmonary vaccination and enhances protection against Mycobacterium tuberculosis. Mucosal Immunol. 2019; 12:805–815. https://doi.org/10.1038/s41385-019-0148-2 PMID: 30778118

30. Van Dis E, Sogi KM, Rae CS, Sivick KE, Surh NH, Leong ML, et al. STING-Activating Adjuvants Elicit a Th17 Immune Response and Protect against Mycobacterium tuberculosis Infection. Cell Rep. 2018; 23:1435–1447. https://doi.org/10.1016/j.celrep.2018.04.003 PMID: 29719256

31. Wang M, Xu G, Lü L, Xu K, Chen Y, Pan H, et al. Genetic polymorphisms of IL-17A, IL-17F, TLR4 and miR-146a in association with the risk of pulmonary tuberculosis. Scientific Reports. 2016; 6:28586. https://doi.org/10.1038/srep28586 PMID: 27339100

32. Zhao J, Wen C, Li M. Association Analysis of Interleukin-17 Gene Polymorphisms with the Risk Susceptibility to Tuberculosis. Lung. Springer US; 2016; 194:459–467. https://doi.org/10.1007/s00408-016-9860-9 PMID: 26899623

33. Manabe YC, Dannenberg AM, Tyagi SK, Hatem CL, Yoder M, Woolwine SC, et al. Different strains of Mycobacterium tuberculosis cause various spectrums of disease in the rabbit model of tuberculosis. Infect Immun. 2003; 71:6004–6011. https://doi.org/10.1128/iai.71.10.6004-6011.2003 PMID: 14500521

34. Yu L, Esser MT, Falloon J, Villafana T, Yang H. Generalized ROC methods for immunogenicity data analysis of vaccine phase I studies in a seropositive population. Human Vaccines & Immunotherapeutics. 2018; 14:2692–2700. https://doi.org/10.1080/21645515.2018.1489191 PMID: 29913105

35. Gengenbacher M, Nieuwenhuizen N, Vogelzang A, Liu H, Kaiser P, Schuerer S, et al. Deletion of nuoG from the Vaccine Candidate Mycobacterium bovis BCG ΔureC::hly Improves Protection against Tuberculosis. Rappuoli R, editor. mBio. American Society for Microbiology; 2016; 7:201. https://doi.org/10.1128/mBio.00679-16 PMID: 27222470

36. Kagina BMN, Tameris MD, Geldenhuys H, Hatherill M, Abel B, Hussey GD, et al. The novel tuberculosis vaccine, AERAS-402, is safe in healthy infants previously vaccinated with BCG, and induces dose-dependent CD4 and CD8T cell responses. Vaccine. 2014; 32:5908–5917. https://doi.org/10.1016/j.vaccine.2014.09.001 PMID: 25218194

37. Hoft DF, Xia M, Zhang GL, Blazevic A, Tennant J, Kaplan C, et al. PO and ID BCG vaccination in humans induce distinct mucosal and systemic immune responses and CD4+ T cell transcriptomal molecular signatures. Mucosal Immunol. Nature Publishing Group; 2018; 11:486–495. https://doi.org/10.1038/mi.2017.67 PMID: 28853442

38. Sayes F, Sun L, Di Luca M, Simeone R, Degaiffier N, Fiette L, et al. Strong immunogenicity and cross-reactivity of Mycobacterium tuberculosis ESX-5 type VII secretion: encoded PE-PPE proteins predicts vaccine potential. Cell Host Microbe. 2012; 11:352–363. https://doi.org/10.1016/j.chom.2012.03.003 PMID: 22520463

39. Broset E, Saubi N, Guitart N, Aguilo N, Uranga S, Kilpeläinen A, et al. MTBVAC-Based TB-HIV Vaccine Is Safe, Elicits HIV-T Cell Responses, and Protects against Mycobacterium tuberculosis in Mice. Mol Ther Methods Clin Dev. 2019; 13:253–264. https://doi.org/10.1016/j.omtm.2019.01.014 PMID: 30859110

40. Levillain F, Kim H, Woong Kwon K, Clark S, Cia F, Malaga W, et al. Preclinical assessment of a new live attenuated Mycobacterium tuberculosis Beijing-based vaccine for tuberculosis. Vaccine. 2020; 38:1416–1423. https://doi.org/10.1016/j.vaccine.2019.11.085 PMID: 31862194

41. Darrah PA, Bolton DL, Lackner AA, Kaushal D, Aye PP, Mehra S, et al. Aerosol vaccination with AERAS-402 elicits robust cellular immune responses in the lungs of rhesus macaques but fails to protect against high-dose Mycobacterium tuberculosis challenge. J Immunol. American Association of Immunologists; 2014; 193:1799–1811. https://doi.org/10.4049/jimmunol.1400676 PMID: 25024382

42. Henao-Tamayo M, Shanley CA, Verma D, Zilavy A, Stapleton MC, Furney SK, et al. The Efficacy of the BCG Vaccine against Newly Emerging Clinical Strains of Mycobacterium tuberculosis. Scriba TJ, editor. PLoS ONE. Public Library of Science; 2015; 10:e0136500. https://doi.org/10.1371/journal.pone.0136500 PMID: 26368806

43. Darrah PA, Zeppa JJ, Maiello P, Hackney JA, Wadsworth MH, Hughes TK, et al. Prevention of tuberculosis in macaques after intravenous BCG immunization. Nature. Nature Publishing Group; 2020; 577:95–102. https://doi.org/10.1038/s41586-019-1817-8 PMID: 31894150

44. Arbues A, Aguilo JI, Gonzalo-Asensio J, Marinova D, Uranga S, Puentes E, et al. Construction, characterization and preclinical evaluation of MTBVAC, the first live-attenuated M. tuberculosis-based vaccine to enter clinical trials. Vaccine. 2013; 31:4867–4873. https://doi.org/10.1016/j.vaccine.2013.07.051 PMID: 23965219

45. Kamath AT, Fruth U, Brennan MJ, Dobbelaer R, Hubrechts P, Ho MM, et al. New live mycobacterial vaccines: the Geneva consensus on essential steps towards clinical development. 2005. pp. 3753–3761.

46. Martín C, Williams A, Hernández-Pando R, Cardona PJ, Gormley E, Bordat Y, et al. The live Mycobacterium tuberculosis phoP mutant strain is more attenuated than BCG and confers protective immunity against tuberculosis in mice and guinea pigs. Vaccine. 2006; 24:3408–3419. https://doi.org/10.1016/j.vaccine.2006.03.017 PMID: 16564606

47. Lanoix J-P, Lenaerts AJ, Nuermberger EL. Heterogeneous disease progression and treatment response in a C3HeB/FeJ mouse model of tuberculosis. Dis Model Mech. 2015; 8:603–610. https://doi.org/10.1242/dmm.019513 PMID: 26035868

48. Henao-Tamayo M, Obregón-Henao A, Creissen E, Shanley C, Orme I, Ordway DJ. Differential Mycobacterium bovis BCG Vaccine-Derived Efficacy in C3Heb/FeJ and C3H/HeOuJ Mice Exposed to a Clinical Strain of Mycobacterium tuberculosis. Burns DL, editor. Clinical and Vaccine Immunology. American Society for Microbiology; 2014; 22:91–98. https://doi.org/10.1128/CVI.00466-14 PMID: 25392011

49. Zhang L, Ru H-W, Chen F-Z, Jin C-Y, Sun R-F, Fan X-Y, et al. Variable Virulence and Efficacy of BCG Vaccine Strains in Mice and Correlation With Genome Polymorphisms. Mol Ther. 2016; 24:398–405. https://doi.org/10.1038/mt.2015.216 PMID: 26643797

50. Coscolla M, Copin R, Sutherland J, Gehre F, de Jong B, Owolabi O, et al. M. tuberculosis T Cell Epitope Analysis Reveals Paucity of Antigenic Variation and Identifies Rare Variable TB Antigens. Cell Host Microbe. 2015; 18:538–548. https://doi.org/10.1016/j.chom.2015.10.008 PMID: 26607161

51. Carpenter SM, Nunes-Alves C, Booty MG, Way SS, Behar SM. A Higher Activation Threshold of Memory CD8+ T Cells Has a Fitness Cost That Is Modified by TCR Affinity during Tuberculosis. Salgame P, editor. PLoS Pathog. 2016; 12:e1005380. https://doi.org/10.1371/journal.ppat.1005380 PMID: 26745507

52. Patankar YR, Sutiwisesak R, Boyce S, Lai R, Lindestam Arlehamn CS, Sette A, et al. Limited recognition of Mycobacterium tuberculosis-infected macrophages by polyclonal CD4 and CD8 T cells from the lungs of infected mice. Mucosal Immunol. Nature Publishing Group; 2020; 13:140–148. https://doi.org/10.1038/s41385-019-0217-6 PMID: 31636345

53. Monin L, Griffiths KL, Slight S, Lin Y, Rangel-Moreno J, Khader SA. Immune requirements for protective Th17 recall responses to Mycobacterium tuberculosis challenge. Mucosal Immunol. 2015; 8:1099–1109. https://doi.org/10.1038/mi.2014.136 PMID: 25627812

54. Gopal R, Monin L, Slight S, Uche U, Blanchard E, Fallert Junecko BA, et al. Unexpected role for IL-17 in protective immunity against hypervirulent Mycobacterium tuberculosis HN878 infection. PLoS Pathog. 2014; 10:e1004099. https://doi.org/10.1371/journal.ppat.1004099 PMID: 24831696

55. Gopal R, Rangel-Moreno J, Slight S, Lin Y, Nawar HF, Fallert Junecko BA, et al. Interleukin-17-dependent CXCL13 mediates mucosal vaccine-induced immunity against tuberculosis. Mucosal Immunol. 2013; 6:972–984. https://doi.org/10.1038/mi.2012.135 PMID: 23299616

56. Flynn JL, Chan J, Triebold KJ, Dalton DK, Stewart TA, Bloom BR. An essential role for interferon gamma in resistance to Mycobacterium tuberculosis infection. J Exp Med. 1993; 178:2249–2254. https://doi.org/10.1084/jem.178.6.2249 PMID: 7504064

57. Tameris MD, Hatherill M, Landry BS, Scriba TJ, Snowden MA, Lockhart S, et al. Safety and efficacy of MVA85A, a new tuberculosis vaccine, in infants previously vaccinated with BCG: a randomised, placebo-controlled phase 2b trial. Lancet. 2013; 381:1021–1028. https://doi.org/10.1016/S0140-6736(13)60177-4 PMID: 23391465

58. Blank CU, Haining WN, Held W, Hogan PG, Kallies A, Lugli E, et al. Defining 'T cell exhaustion". Nat Rev Immunol. Nature Publishing Group; 2019; 14:768–10. https://doi.org/10.1038/s41577-019-0221-9 PMID: 31570879

59. Sakai S, Kauffman KD, Schenkel JM, McBerry CC, Mayer-Barber KD, Masopust D, et al. Cutting Edge: Control of Mycobacterium tuberculosis Infection by a Subset of Lung Parenchyma-Homing CD4 T Cells. The Journal of Immunology. 2014; 192:2965–2969. https://doi.org/10.4049/jimmunol.1400019 PMID: 24591367

60. Moguche AO, Musvosvi M, Penn-Nicholson A, Plumlee CR, Mearns H, Geldenhuys H, et al. Antigen Availability Shapes T Cell Differentiation and Function during Tuberculosis. Cell Host Microbe. 2017; 21:695–706.e5. https://doi.org/10.1016/j.chom.2017.05.012 PMID: 28618268

61. Larocca RA, Provine NM, Aid M, Iampietro MJ, Borducchi EN, Badamchi-Zadeh A, et al. Adenovirus serotype 5 vaccine vectors trigger IL-27-dependent inhibitory CD4+ T cell responses that impair CD8+ T cell function. Sci Immunol. 2016; 1:eaaf7643–eaaf7643. https://doi.org/10.1126/sciimmunol.aaf7643 PMID: 28239679

62. Ardain A, Domingo-Gonzalez R, Das S, Kazer SW, Howard NC, Singh A, et al. Group 3 innate lymphoid cells mediate early protective immunity against tuberculosis. Nature. 2019; 570:528–532. https://doi.org/10.1038/s41586-019-1276-2 PMID: 31168092

63. Coulter F, Parrish A, Manning D, Kampmann B, Mendy J, Garand M, et al. IL-17 Production from T Helper 17, Mucosal-Associated Invariant T, and γδ Cells in Tuberculosis Infection and Disease. Front Immunol. 2017; 8:1252. https://doi.org/10.3389/fimmu.2017.01252 PMID: 29075255

64. Dijkman K, Sombroek CC, Vervenne RAW, Hofman SO, Boot C, Remarque EJ, et al. Prevention of tuberculosis infection and disease by local BCG in repeatedly exposed rhesus macaques. Nat Med. 2019; 25:255–262. https://doi.org/10.1038/s41591-018-0319-9 PMID: 30664782

65. Provine NM, Larocca RA, Penaloza-MacMaster P, Borducchi EN, McNally A, Parenteau LR, et al. Longitudinal requirement for CD4+ T cell help for adenovirus vector-elicited CD8+ T cell responses. The Journal of Immunology. 2014; 192:5214–5225. https://doi.org/10.4049/jimmunol.1302806 PMID: 24778441

66. Rohart F, Gautier B, Singh A, Lê Cao K-A. mixOmics: An R package for 'omics feature selection and multiple data integration. PLoS Comput Biol. 2017; 13:e1005752. https://doi.org/10.1371/journal.pcbi.1005752 PMID: 29099853